

RESEARCH

Open Access



Regulation of vascular endothelial integrity by mesenchymal stem cell extracellular vesicles after hemorrhagic shock and trauma

Mark Barry¹ , Alpa Trivedi², Byron Miyazawa², Lindsay R. Vivona², David Shimmin³, Praneeti Pathipati², Callie Keane², Joseph Cuschieri¹ and Shibani Pati^{1,2*}

Abstract

Background Patients with hemorrhagic shock and trauma (HS/T) are vulnerable to the endotheliopathy of trauma (EOT), characterized by vascular barrier dysfunction, inflammation, and coagulopathy. Cellular therapies such as mesenchymal stem cells (MSCs) and MSC extracellular vesicles (EVs) have been proposed as potential therapies targeting the EOT. In this study we investigated the effects of MSCs and MSC EVs on endothelial and epithelial barrier integrity *in vitro* and *in vivo* in a mouse model of HS/T. This study addresses the systemic effects of HS/T on multiorgan EOT.

Methods *In vitro*, pulmonary endothelial cell (PEC) and Caco-2 intestinal epithelial cell monolayers were treated with control media, MSC conditioned media (CM), or MSC EVs in varying doses and subjected to a thrombin or hydrogen peroxide (H₂O₂) challenge, respectively. Monolayer permeability was evaluated with a cell impedance assay, and intercellular junction integrity was evaluated with immunofluorescent staining. *In vivo*, a mouse model of HS/T was used to evaluate the effects of lactated Ringer's (LR), MSCs, and MSC EVs on endothelial and epithelial intercellular junctions in the lung and small intestine as well as on plasma inflammatory biomarkers.

Results MSC EVs and MSC CM attenuated permeability and preserved intercellular junctions of the PEC monolayer *in vitro*, whereas only MSC CM was protective of the Caco-2 epithelial monolayer. *In vivo*, both MSC EVs and MSCs mitigated the loss of endothelial adherens junctions in the lung and small intestine, though only MSCs had a protective effect on epithelial tight junctions in the lung. Several plasma biomarkers including MMP8 and VEGF were elevated in LR- and EV-treated but not MSC-treated mice.

Conclusions In conclusion, MSC EVs could be a potential cell-free therapy targeting endotheliopathy after HS/T via preservation of the vascular endothelial barrier in multiple organs early after injury. Further research is needed to better understand the immunomodulatory effects of these products following HS/T and to move toward translating these therapies into clinical studies.

Keywords Mesenchymal stem cells, Mesenchymal stem cell extracellular vesicles, Hemorrhagic shock, Trauma

*Correspondence:

Shibani Pati
Shibani.Pati@ucsf.edu

¹ Department of Surgery, University of California, San Francisco, 513 Parnassus Ave, San Francisco, CA 94143, USA

² Department of Laboratory Medicine, University of California, San Francisco, 513 Parnassus Ave, San Francisco, CA 94143, USA

³ NanoCraft.US., 807 Aldo Ave, Suite-101, Santa Clara, CA 95054, USA



© The Author(s) 2024. **Open Access** This article is licensed under a Creative Commons Attribution 4.0 International License, which permits use, sharing, adaptation, distribution and reproduction in any medium or format, as long as you give appropriate credit to the original author(s) and the source, provide a link to the Creative Commons licence, and indicate if changes were made. The images or other third party material in this article are included in the article's Creative Commons licence, unless indicated otherwise in a credit line to the material. If material is not included in the article's Creative Commons licence and your intended use is not permitted by statutory regulation or exceeds the permitted use, you will need to obtain permission directly from the copyright holder. To view a copy of this licence, visit <http://creativecommons.org/licenses/by/4.0/>. The Creative Commons Public Domain Dedication waiver (<http://creativecommons.org/publicdomain/zero/1.0/>) applies to the data made available in this article, unless otherwise stated in a credit line to the data.

Background

Patients with severe injuries and hemorrhagic shock are susceptible to the endotheliopathy of trauma (EOT), which includes vascular barrier compromise, systemic inflammation, and dysfunctional coagulation [1–3]. The EOT is closely linked with multiple organ failure and contributes to increased mortality after injury [4, 5]. While plasma-based resuscitation and modern trauma systems have improved outcomes in severely injured patients [6, 7], trauma remains a leading cause of death in the United States [8], and novel therapies are needed.

Bone marrow derived mesenchymal stem cells (MSCs) are known to have vasculoprotective, anti-inflammatory, and regenerative properties and are the focus of numerous ongoing clinical trials [9, 10]. In light of these properties, MSCs have been proposed as a potential therapy targeting the EOT and have been shown to reduce injury in multiple organs [11–14] and reverse bone marrow suppression [15] in rodent models of hemorrhagic shock and trauma (HS/T). Though initially MSCs were thought to act through their ability to home to injured tissue, the majority of intravenously administered MSCs become trapped in capillary networks such as in the lungs; one of their primary mechanisms of action is now understood to be through the release of bioactive soluble factors and extracellular vesicles (EVs) [10, 16, 17]. EVs are membrane-bound particles containing RNA, DNA, protein, and lipids from their parent cells and are highly effective mediators of intercellular communication [18]. MSC EVs have been proposed as a “cell-free” therapy as they have been shown to recapitulate the therapeutic properties of MSCs [17, 19].

We recently demonstrated in a mouse model of HS/T that both MSCs and MSC EVs mitigate histologic injury and vascular permeability to a 10 kDa dextran dye in the small intestine and lungs [12]. The purpose of the current study was to further investigate the molecular mechanism of MSCs and MSC EVs in HS/T, specifically their effects on endothelial and epithelial barrier integrity and on systemic inflammatory biomarkers. We hypothesized that MSCs and MSC EVs would (1) preserve pulmonary endothelial and intestinal epithelial barrier integrity *in vitro* and (2) preserve intercellular junctions in the small intestine and lungs and reduce plasma inflammatory biomarker levels *in vivo*.

Methods

Mesenchymal stem cell culture and EV isolation

Human bone marrow-derived MSCs (passage 1) were obtained from Rooster Bio Inc. (Frederick, MD) and expanded initially on a Terumo Quantum Device (Terumo, Lakewood, CO) to generate passage 2 cells that were used in all studies. MSCs were grown in

Mesenchymal Stem Cell Growth Medium 2 (PromoCell, Heidelberg, Germany) and maintained at 37 °C and 5% CO₂ in a humidified incubator. To isolate MSC EVs, the MSCs were grown to 80% confluence, then serum-starved for 48 h. The MSC conditioned media (CM) was collected and centrifuged at 1500g × 10 min to remove cellular debris, then filtered using a 0.22 μm filter. EVs were isolated from the MSC CM using a Tangential Flow Filtration System with the Pellicon[®] XL50 Cassette with Biomax[®] 500 kDa Membrane (MilliporeSigma, Burlington, MA). A subset of the isolated EVs were further concentrated using an Amicon Ultra-2 Centrifugal Filter 3K Device (MilliporeSigma) according to manufacturer instructions for use in the *in vitro* experiments. Aliquots of isolated EVs were stored at -80 °C. The MSC EVs used in this study were characterized by flow cytometry, nanoparticle tracking analysis, and spectrophotometry as previously described [12], and scanning electron microscopy images were also captured for this study (Supplemental Figure 1).

Pulmonary endothelial cell (PEC) and Caco-2 intestinal epithelial cell culture

Human pulmonary microvascular endothelial cells (PECs) were obtained from PromoCell and grown in Endothelial Cell Growth Medium MV2 (PromoCell). Passages 3–7 were used in all experiments. Caco-2 human intestinal epithelial cells were obtained from American Type Culture Collection (ATCC, Manassas, VA) and were grown in Eagle's Minimum Essential Medium (ATCC) supplemented with 20% Fetal Bovine Serum and 1% penicillin/streptomycin. Passages 2–5 were used in all experiments. Both cell lines were maintained at 37 °C and 5% CO₂ in a humidified incubator.

In vitro pulmonary endothelial cell (PEC) monolayer barrier integrity and intercellular junction immunostaining

Pulmonary endothelial cell (PEC) monolayer barrier integrity was measured *in vitro* using an electric cell-substrate impedance sensing system (ECIS 1600, Applied BioPhysics, Troy, NY). To evaluate the PEC monolayer, PECs (50,000 cells per well) were seeded onto a 96-well plate containing electrodes that had been pre-treated with L-cysteine and were grown to confluence. The PEC monolayers were serum-starved for one hour and once resistances had stabilized were then pre-treated with MSC control media (10% or 20% v/v), MSC CM (10% or 20% v/v), or MSC EVs (10 or 30 μg/ml). We used MSC CM rather than MSCs in these *in vitro* experiments as the CM contains all of the soluble factors and EVs that MSCs produce without having to administer live MSCs which would confound resistance readings within the well. In addition, the estimated amount of EVs in the

MSC CM is comparable to the amount in the MSC EV groups at these doses. Because the MSC EVs were more concentrated, a smaller treatment volume was required compared to the MSC CM or MSC control media. We did not concentrate the MSC CM in order to pre-treat the cell monolayers with equivalent volumes, as this would concentrate all other soluble factors in the MSC CM such as growth factors which may be harmful to the cell monolayers. After 30 min the PEC monolayers were challenged with thrombin at 0.2 μ /ml to induce paracellular permeability. Note that the PEC monolayers were treated with MSC control media, CM, or MSC EVs prior to thrombin administration because the onset of cell permeability following the addition of thrombin is extremely rapid. Resistances were measured in 5-min intervals at 4000 Hz. Data were normalized to the mean resistance of the monolayers before the treatments. Resistance tracings and area under the curve (AUC) plots were generated for each treatment group to compare monolayer integrity.

To evaluate intercellular junction integrity of the PEC monolayer, PECs were separately grown on cover slips (coated with collagen type 1) in 24-well plates (50,000 cells per well). The wells were pre-treated with MSC control media (10% or 20% v/v), MSC CM (10% or 20% v/v) or MSC EVs (30 μ g/ml) for 30 min then challenged with thrombin 0.2 μ /ml. 5 min after the addition of thrombin, the cells were washed three times with PBS then fixed with 4% PFA. Immunostaining was then performed using antibodies against VE-cadherin (Cell Signaling, Danvers, MA) and Zonula Occludens-1 (ZO-1, Abcam, Burlingame, CA). F-actin was detected with Texas Red Phalloidin (Cell Signaling). Representative images were captured using a Nikon Eclipse 80i microscope (Nikon, Melville, NY) with an RT-scmos camera (SPOT Imaging, Sterling Heights, MI).

In vitro Caco-2 intestinal epithelial cell monolayer barrier integrity and intercellular junction immunostaining

To evaluate the Caco-2 intestinal epithelial monolayer, Caco-2 cells (25,000 cells per well) were seeded onto a 96-well plate for ECIS as above and grown to confluence. The Caco-2 monolayers were serum-starved for 2 h and once resistances had stabilized were then pre-treated with MSC control media (10% or 25% v/v), MSC CM (10% or 25% v/v), or MSC EVs (10, 30, or 50 μ g/ml). After 30 min the Caco-2 cell monolayers were challenged with hydrogen peroxide (H_2O_2) at 2.5 mM to cause oxidative stress; this dose was chosen based on preliminary studies in the lab showing decreased resistance across the monolayer in this model. Note that the Caco-2 monolayers were treated with MSC control media, CM, or MSC EVs prior to H_2O_2 administration because the onset of cell

permeability following the addition of H_2O_2 is extremely rapid. Resistances were measured in 4-min intervals at 1000 Hz. Data normalization, resistance tracings, and AUC plot generation were conducted as above.

To evaluate intercellular junction integrity of the Caco-2 monolayer, Caco-2 cells were separately seeded on to 24-well plates (80,000 cells per well). The cells were pre-treated with MSC control media (10% or 25% v/v), MSC CM (10% or 25% v/v) or MSC EVs (30 μ g/ml) for 30 min then challenged with H_2O_2 2.5 mM. 2.5 h after exposure to H_2O_2 , the cells were washed three times with PBS then fixed with 4% PFA. Immunostaining was then performed using antibody against ZO-1 (Abcam), and F-actin was detected using Texas Red Phalloidin (Cell Signaling). Representative images were captured using a Revolve microscope (Echo Inc., San Diego, CA).

Animal studies

Animal studies were performed with approval of the Institutional Animal Care and Use Committee (IACUC) at UCSF. The experiments were conducted in compliance with the ARRIVE guidelines for animal models and the National Institutes of Health (NIH) guidelines on the use of laboratory animals. All animals were housed in a room with access to food and water ad libitum, controlled temperature, and 12:12-h light–dark cycles.

Mouse model of hemorrhagic shock and trauma

Male C57BL6 mice, 8–12 weeks old, were obtained from The Jackson Laboratory (Sacramento, CA) (N=20 total). Mice underwent an established model of HS/T [12, 20, 21]. Briefly, the mice were anesthetized with isoflurane and maintained at a body temperature between 35 °C and 37 °C using a heating plank. The bilateral femoral arteries were cannulated with heparinized catheters, one for continuous blood pressure monitoring (PowerLab 7, AD Instruments, Dunedin, New Zealand), and the other for blood withdrawal and resuscitation. A 2 cm midline laparotomy was also performed to induce additional trauma. Mice were subsequently bled to a mean arterial pressure (MAP) of 35 mmHg for 90 min and then resuscitated with a 200 μ L fluid bolus containing (1) lactated Ringer's (LR), (2) 1×10^6 MSCs in LR, or (3) MSC EVs (30 μ g) in PBS. These doses were chosen based on previous work demonstrating efficacy of MSC and MSC EVs in this model [12, 21]. Sham mice underwent cannulation without laparotomy or hemorrhage. Mice were monitored hemodynamically for an additional 30 min after resuscitation. Two hours post-resuscitation, the mice were re-anesthetized with isoflurane. Blood was collected via cardiac puncture and the mice were perfused with 10 ml of ice-cold PBS. Sodium citrate 3.2% was added to the blood in a 1:9 ratio prior to centrifugation at 3000 g for

10 min to isolate the plasma fraction, which was stored at -80°C . The lungs and a segment of small intestine were harvested and flash-frozen in isopentane and stored at -80°C .

Intercellular junction immunostaining of the small intestine and lungs

The lungs and small intestine from $N=5$ mice per group were sectioned at $10\ \mu\text{m}$ thickness. The sections were fixed in ice-cold 95% EtOH for 20 min then 100% acetone for 1 min. Immunostaining was then performed using antibodies against the adherens junction protein VE-cadherin (R&D Systems, Minneapolis, MN) and the tight junction proteins ZO-1 (Abcam, Burlingame, CA) and claudin-4 (Thermo Fisher, Waltham, MA). Sections were imaged in a blinded fashion with a Nikon Eclipse 80i microscope (Nikon) with an RT-scmos camera (SPOT Imaging), and representative images were selected from each animal for qualitative comparison.

Plasma inflammatory biomarker analysis

Mouse plasma samples ($N=5$ per group) were analyzed using a custom multiplex Luminex[®] Discovery Assay Kit (R&D Systems, Minneapolis, MN) according to the manufacturer's protocol. The following analytes were included: Angiopoietin-2 (Ang-2), C-X-C Motif Chemokine Ligand 10 (CXCL10), CXCL12, Intercellular Adhesion Molecule-1 (ICAM-1), Interferon gamma (IFN- γ), Interleukin-1beta (IL-1 β), IL-2, IL-4, IL-6, IL-6 receptor alpha (IL-6Ra), IL-10, Matrix Metalloproteinase-8 (MMP8), MMP9, Syndecan-1, Tumor Necrosis Factor alpha (TNF α), TNF Receptor Superfamily Member 1a (TNFRSF1a), TNFRSF1b, TNF Superfamily Member 13b (TNFSF13b), and Vascular Endothelial Growth Factor (VEGF). Plasma samples were thawed and centrifuged at 16,000 g for 4 min prior to use. Samples were then diluted 1:2 and 1:10 in appropriate diluent and pipetted onto a 96-well plate, mixed with magnetic beads coated with antibodies, and incubated for 2 h at room temperature on a horizontal orbital microplate shaker at 800 rpm. Three washes with wash buffer were performed, then the beads were incubated with the biotinylated antibody cocktail for 1 h at room temperature on the orbital shaker at 800 rpm. After another three washes, the beads were incubated with streptavidin-PE for 30 min on the shaker. The beads were washed a final three times then resuspended in wash buffer prior to being read on a MAGPIX System (Luminex Corp., Austin, TX). xPONENT 4.2 software (Luminex Corp.) was used for data acquisition.

Statistical analysis

Area under the curve values for the in vitro experiments were compared using one-way ANOVA with Tukey's

post hoc tests. Mean arterial pressures (MAPs) were compared using repeated measures two-way ANOVA with Tukey's multiple comparisons test. For the plasma biomarker analysis, first outliers were removed using the ROUT method in Prism 9.0 (GraphPad Inc., San Diego, CA), and data were assessed for normality using the Shapiro-Wilk test. One-way ANOVA with post-hoc Tukey's test was used for normally distributed data, and Kruskal-Wallis testing with Dunn's multiple comparisons test was used for data that did not pass the normality testing. $p < 0.05$ was considered significant. All analyses were performed using Prism 9.0. Data in this manuscript are presented as mean \pm SD.

Results

MSC EV characterization

The MSC EVs used in this study have been characterized previously by nanoparticle tracking analysis, spectrophotometry, and flow cytometry [12]. The EVs had a concentration of 1.16×10^9 particles/ml with a size peak at 123 nm and protein content of 160 $\mu\text{g/ml}$. A subset of the EVs further concentrated for the in vitro experiments had a protein content of 330 $\mu\text{g/ml}$. By flow cytometry the EVs were positive for EV-specific markers CD69, CD81 and CD9, MSC markers CD73 and CD90, and negative for negative control markers CD31, CD45, and HLA-DR. In addition, images of the MSC EVs via scanning electron microscopy were obtained, consistent with the particle size demonstrated via nanoparticle tracking analysis (Supplemental Figure 1).

MSC conditioned media and MSC EVs protect the pulmonary endothelial barrier in vitro

Resistance tracings generated by ECIS and AUC calculations demonstrated a drop in resistance across PEC monolayers exposed to thrombin, indicating increased paracellular permeability (Fig. 1A, B). MSC CM refers to cell culture media containing the MSC secretome, whereas MSC control media has not been exposed to MSCs and thus does not contain MSC-secreted factors or EVs. Cell monolayers that had been pre-treated with MSC CM had significantly higher resistances than those treated with MSC control media at both of the tested doses. The higher dose of MSC EVs at 30 $\mu\text{g/ml}$ was also protective.

Consistent with the ECIS tracings, immunostaining for the tight junction protein ZO-1 and adherens junction protein VE-cadherin demonstrated a loss of ZO-1 and VE-cadherin staining among PEC monolayers exposed to thrombin (Fig. 1C). In addition, thrombin exposure resulted in gap formation or separation between cells. Pre-treatment with MSC CM or MSC EVs resulted in relative preservation of PEC barrier integrity as evidenced

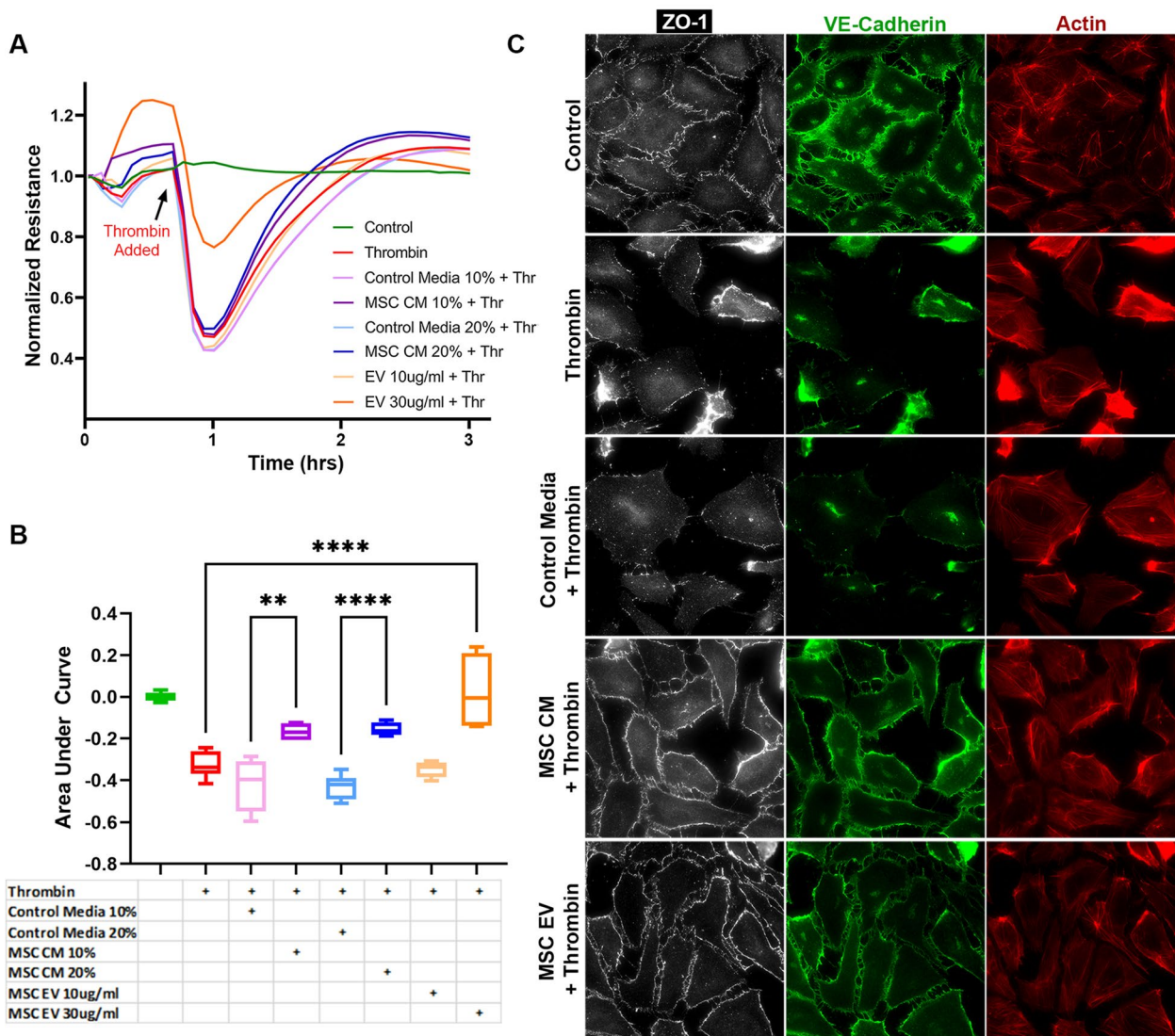


Fig. 1 Effects of MSC CM and MSC EVs on a Pulmonary Endothelial Cell Monolayer in Vitro. **A** Pulmonary endothelial cell (PEC) monolayer resistance tracings at 4000Hz in response to thrombin challenge. N=4 cell replicates per group. **B** Area under the curve (AUC) plot for resistances following the addition of thrombin. **p < 0.01, ****p < 0.0001 by one-way ANOVA with post-hoc Tukey's tests. **C** Representative images (40x magnification) of immunofluorescence staining of PEC monolayers for Zonula Occludens-1 (ZO-1, white), VE-cadherin (green), and Actin (red). The addition of thrombin caused decreased resistance across the monolayer as well as loss of ZO-1 and VE-cadherin staining and gap formation with cells. Pre-treatment of the cell monolayers with MSC CM (20%) or MSC EVs (30 µg/ml) partially attenuated these effects, whereas MSC control media (20%) was not protective

by attenuation of the loss of ZO-1 and VE-cadherin staining and decreased gap formation. F-actin staining of the PEC monolayer showed reduced stress fiber activation when compared to the thrombin challenged group.

MSC conditioned media but not MSC EVs protect the intestinal epithelial barrier in vitro

Caco-2 intestinal epithelial cell monolayers exhibited decreased resistance, or increased permeability, in

response to H₂O₂ exposure (Fig. 2A, B). MSC CM was significantly protective compared to control media at the higher dose (25%) tested. However, MSC EV pre-treatment was not protective at any of the tested doses. Immunostaining was also performed on the Caco-2 monolayers to evaluate ZO-1 and actin (Fig. 2C). H₂O₂ exposure resulted in re-distribution of actin filaments and decreased ZO-1 staining compared to control conditions. Pre-treatment with MSC CM preserved actin organization and attenuated the loss of ZO-1. However,

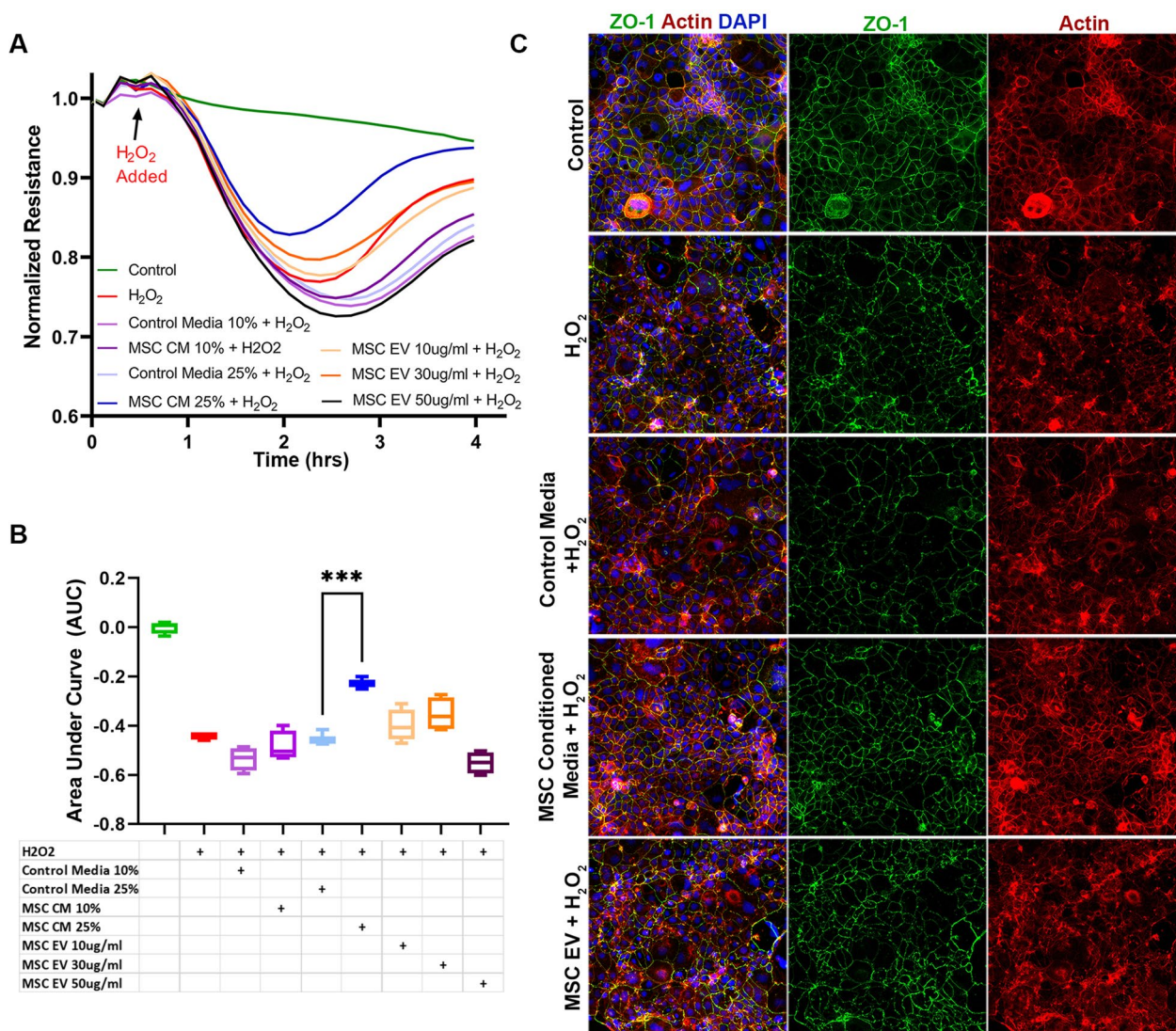


Fig. 2 Effects of MSC CM and MSC EVs on the Caco-2 Intestinal Epithelial Cell Monolayer in Vitro. **A** Caco-2 intestinal epithelial cell resistance tracings at 1000Hz in response to H₂O₂ challenge. N=4 cell replicates per group. **B** Area under the curve (AUC) plot for resistances following the addition of H₂O₂. ***p < 0.001 by one-way ANOVA with post-hoc Tukey's tests. **C** Representative images (10× magnification) of immunofluorescence staining of Caco-2 monolayers for Zonula Occludens-1 (ZO-1, green), Actin (red), and DAPI (blue). The addition of H₂O₂ caused decreased resistance across the monolayer as well as relative loss of ZO-1 staining and actin redistribution. MSC CM (25%) pre-treatment decreased the effects of H₂O₂, whereas treatment with MSC control media (25%) or MSC EVs (30 μg/ml) were not protective

similar to the results demonstrated by ECIS, MSC EV pre-treatment did not affect ZO-1 or actin staining.

MSCs and MSC EVs preserve endothelial adherens junctions in the intestine and lung in vivo

The HS/T model schematic is depicted in Fig. 3. Mean arterial pressures (MAPs) were similar among mice resuscitated with LR, MSCs, or MSC EVs. Sections of the lungs and small intestine of mice subjected to HS/T were stained to evaluate endothelial and epithelial barrier integrity in vivo. In the lungs, HS/T with LR

resuscitation induced a qualitative loss of VE-cadherin (adherens junction) staining among endothelial-lined blood vessels and alveolar capillaries compared to sham mice. MSC and MSC EV treatment resulted in relative preservation of VE-cadherin staining. Moreover, there was notable compromise of ZO-1 (tight junction) staining in the epithelial-lined airways that underwent HS/T compared to sham mice, however this finding was partially mitigated in the MSC group. There was also loss of ZO-1 staining in the alveoli regardless of treatment group after HS/T (Fig. 4). In the small intestine,

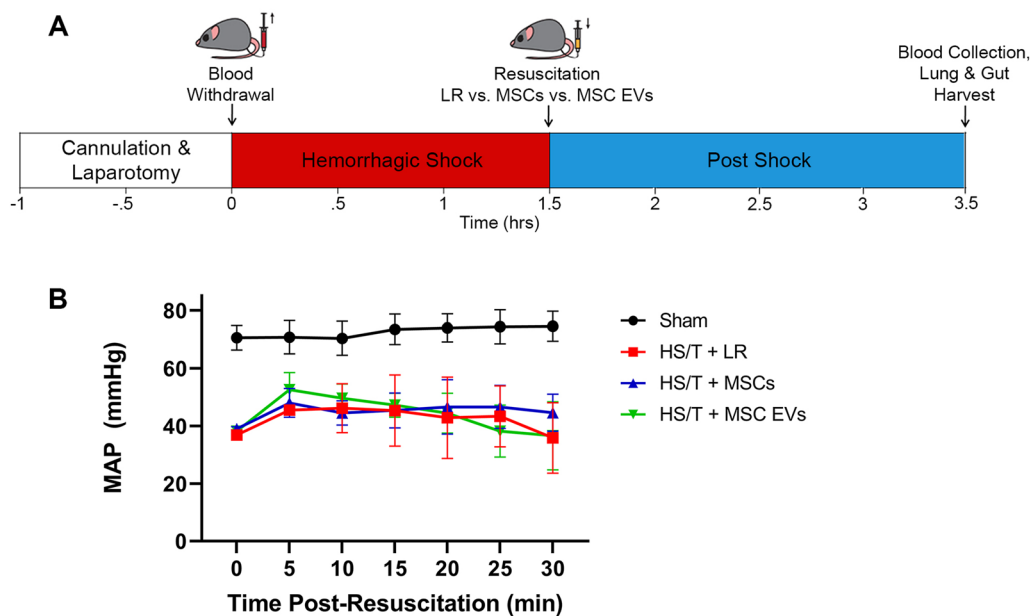


Fig. 3 Hemorrhagic Shock and Trauma Mouse Model. **A** Depiction of the 90-min HS/T model. Mice were resuscitated with LR, MSCs, or MSC EVs (N = 5 mice per group). Blood collection and organ harvest were performed 2 h after the end of shock. **B** Mean arterial pressures (MAPs) during the 30 min post-resuscitation. There was no effect of resuscitation group on MAPs ($p=0.74$) by two-way ANOVA with repeated measures

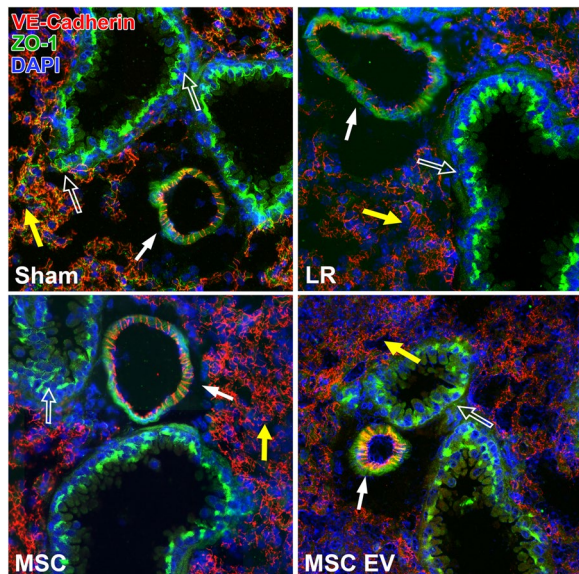


Fig. 4 Intercellular Junction Staining in the Lung after Hemorrhagic Shock and Trauma (HS/T). Representative images (20 \times magnification) of lungs stained for VE-cadherin (endothelial adherens junctions; red), ZO-1 (tight junctions; green), and DAPI (nuclei; blue). Mice subjected to HS/T and resuscitated with LR demonstrate loss of ZO-1 staining between epithelial cells in the airways as well as in the alveolar epithelium. LR-resuscitated mice also demonstrate a loss of staining for VE-cadherin in small blood vessels. Treatment with MSCs or MSC EVs restored VE-cadherin staining suggesting a protective effect on endothelial barrier integrity. MSC treatment also partially protected against loss of ZO-1 in the epithelial-lined airways. *Open arrow* points to airway. *Closed arrow* points to blood vessel. *Yellow arrow* points to alveoli containing capillaries and epithelial cells

sections stained for VE-cadherin demonstrated a loss of VE-cadherin staining in the submucosal vessels after HS/T in LR-treated mice, whereas MSC and MSC EV treatment qualitatively preserved VE-cadherin staining in these vessels. Staining for ZO-1 and claudin-4 was also performed to evaluate epithelial integrity, however, there were no substantial differences across the sham or injured groups (Fig. 5).

Plasma biomarker analysis

The levels of each plasma inflammatory biomarker are listed in Table 1. Biomarkers that showed significant differences between any of the groups are depicted in Fig. 6. Compared to sham mice, LR-treated mice had significantly higher levels of IL-10, MMP-8, MMP-9, TNFRSF1b, and VEGF, MSC-treated mice had higher levels of TNFRSF1b and showed a trend toward higher levels of CXCL12 ($p=0.06$), and EV-treated mice had higher levels of IFN- γ , IL-1B, IL-6, IL-10, MMP-8, MMP-9, TNF α , TNFRSF1b, and VEGF and showed a trend toward higher levels of CXCL10 ($p=0.06$) and CXCL12 ($p=0.06$). Other biomarkers were similar across groups. Notably, both MMP-8 and VEGF were significantly elevated among the LR- and EV-treated groups compared to sham mice, whereas these biomarker levels were not significantly different between MSC-treated mice and sham mice.

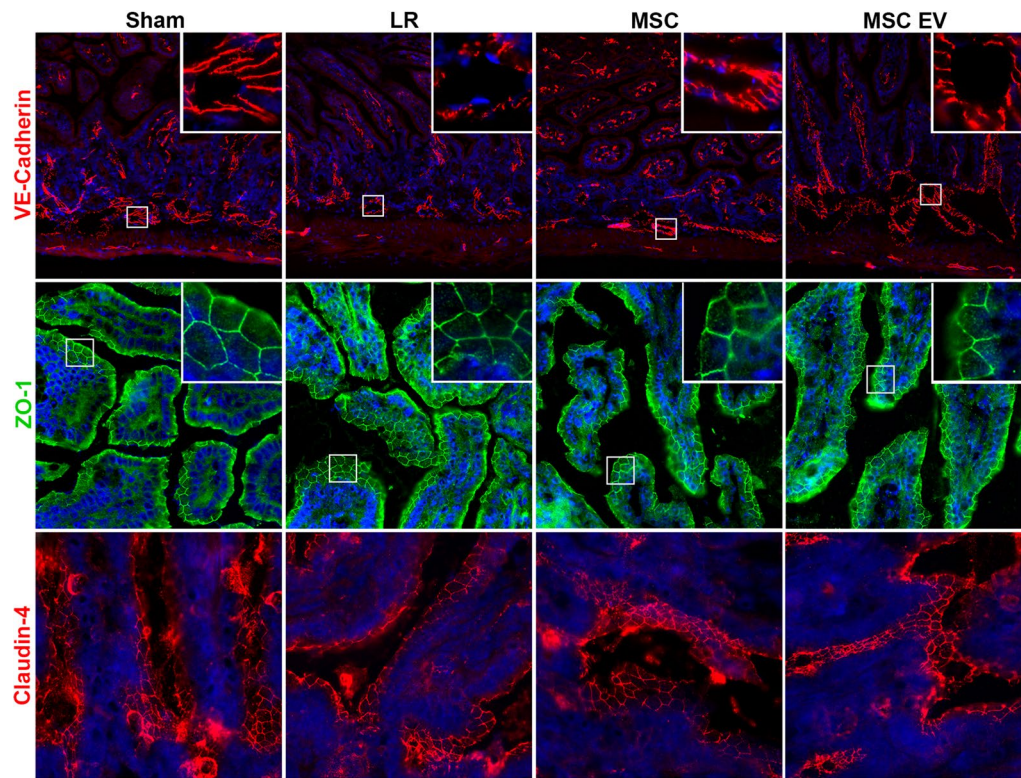


Fig. 5 Intercellular Junction Staining in the Small Intestine after Hemorrhagic Shock and Trauma (HS/T). Representative images of small intestine stained for VE-cadherin (adherens junctions; red; 10× magnification), ZO-1 (tight junctions; green; 20× magnification), claudin-4 (tight junctions; red; 20× magnification), and DAPI (nuclei; blue). LR-treated mice demonstrated a loss of VE-cadherin in the submucosal blood vessels (see 40× image inset) of the small intestine, whereas MSC or MSC EV treatment attenuated this finding. Epithelial barrier integrity was evaluated with ZO-1 and claudin-4 staining, however no differences were evident between groups

Conclusions

Our previous work has shown that MSC EVs recapitulate the ability of MSCs to mitigate histologic injury and vascular permeability in the lungs and small intestine in mice after HS/T. This study further demonstrates that MSCs and MSC EVs may target the EOT via preservation of the vascular endothelial barrier early after injury.

In this study, we demonstrated *in vitro* that both MSCs and MSC EVs preserve barrier properties of a pulmonary endothelial monolayer. While MSC CM also helped to maintain barrier integrity of a Caco-2 intestinal epithelial monolayer, MSC EVs were not protective at multiple tested doses. This finding may be due to higher concentrations of protective factors or additional soluble factors in the MSC CM compared to the MSC EVs. *In vivo* in a mouse model of HS/T, both MSCs and MSC EVs attenuated the loss of endothelial adherens junction staining in blood vessels in the lung and small intestine. MSCs but not MSC EVs resulted in a partial protective effect on epithelial tight junctions in the lung. Epithelial tight junctions in the small intestine were not clearly affected in this model. Altogether these results suggest that one

potential therapeutic mechanism of MSCs and MSC EVs in HS/T is an early protective effect on vascular barrier integrity.

In addition, at two hours post resuscitation, we did find that there were several differences in the inflammatory biomarker profiles between groups. For example, both MMP8 and VEGF were significantly elevated among LR- and EV-treated (but not MSC-treated) mice compared to sham. MMP8 has been shown to be involved in tight junction protein degradation in endothelial cells [22]; and VEGF is known to be a potent vascular permeabilizing agent, acting via multiple mechanisms including phosphorylation and loss of tight and adherens junctions, induction of matrix metalloproteinase expression, and negative regulation of pericyte function [23]. This suggests that there may be some differences in the immunomodulatory effects of MSCs and MSC EVs after HS/T. There were no significant differences seen across groups, however, for a number of the tested biomarkers. It is possible that other time points than the one used in this study may better capture the immunomodulatory effects of MSCs and MSC EVs in this model, as MSCs and MSC

Table 1 Plasma Inflammatory Biomarkers after Hemorrhagic Shock and Trauma

Analyte	Sham (pg/ml)	LR (pg/ml)	MSC (pg/ml)	EV (pg/ml)
Ang2	27,324 ± 3424	23,371 ± 3809	30,293 ± 6566	24,191 ± 5852
CXCL10	0 ± 0	7379 ± 5459	16,318 ± 18,089	28,938 ± 23,111
CXCL12	1472 ± 85.73	1612 ± 75.6	1687 ± 154 ^a	1687 ± 124.7 ^a
ICAM-1	15,294 ± 4666	12,057 ± 3535	12,936 ± 2642	14,130 ± 2570
IFN-γ	0 ± 0	2.68 ± 3.627	0 ± 0	5.46 ± 5.26 ^{a,b}
IL-1β	0 ± 0	104.4 ± 88.06	61.4 ± 104	151.6 ± 130 ^a
IL2	0 ± 0	0.6 ± 1.34	0.72 ± 1.61	2.04 ± 2.82
IL4	330 ± 7.97	324.8 ± 27.58	323.8 ± 36.41	331 ± 23.01
IL6	53.2 ± 35.32	10,198 ± 9560	11,992 ± 16,983	60,396 ± 41279 ^a
IL6Ra	10,349 ± 909.3	10,780 ± 639	11,144 ± 1209	10,399 ± 1529
IL10	3.6 ± 0.55	857.4 ± 461.1 ^a	299 ± 259.8	1229 ± 895.8 ^a
MMP8	282,150 ± 103,143	4,577,903 ± 1649162 ^a	3,615,807 ± 2,199,024	8,471,390 ± 3408584 ^{a,b}
MMP9	10,488 ± 4969	118,897 ± 35588 ^a	94,408 ± 51062 ^a	146,319 ± 59425 ^a
Syndecan-1	8031 ± 3599	9799 ± 1811	12,253 ± 3066	10,605 ± 2461
TNF-α	1.8 ± 0.45	84.4 ± 52.34	60.8 ± 59.78	189.8 ± 126.3 ^a
TNFRSF1a	1075 ± 272.6	5002 ± 3029	4065 ± 2327	5060 ± 3407
TNFRSF1b	3347 ± 854.7	14,819 ± 3996 ^a	14,213 ± 5198 ^a	19,580 ± 3965 ^a
TNFRSF3b	5920 ± 978	5506 ± 802	6253 ± 1194	7120 ± 2088
VEGF	17.6 ± 4.34	144.2 ± 82.35 ^a	116.2 ± 84.53	247.8 ± 57.9 ^{a,b}

Luminex multiplex measurement of plasma from mice at 2 h post-resuscitation. Groups were compared using one-way ANOVA for normally distributed data and Kruskal–Wallis testing for data that were not normally distributed. Outliers were defined by the GraphPad program and were removed from analysis. Numbers are mean ± SD, N=5 mice per group

^a Statistically significant difference compared to sham, ^b Statistically significant difference compared to MSC. p values as indicated in Fig. 6

EVs have been shown to have numerous immune-regulating effects in a variety of inflammatory diseases [25, 26].

Interestingly, TNFα was also elevated in the EV group, a pro-apoptotic and pro-inflammatory cytokine, which makes it challenging to draw conclusions regarding the net effect of these treatments on inflammation after HS/T. While MSCs and MSC EVs are widely understood to have anti-inflammatory effects in various disease processes, others have shown that MSC infusion in mice initially can cause systemic immune activation, later followed by reduced immune reactivity [24]. This further suggests that using additional time points would be beneficial to understanding MSC and MSC EV immunomodulation after HS/T. In particular, if MSCs and MSC EVs do indeed have differing effects on inflammation after HS/T, this could have important clinical consequences. Future studies using this model of HS/T should also evaluate the immunomodulatory effects of these therapies at different doses.

MSCs and MSC EVs contain numerous bioactive factors, including mRNAs, microRNAs, proteins, and lipids, a combination of which may underly the vasculoprotective properties seen in this study. For example, MSCs and MSC EVs contain the mRNA angiopoietin-1 (Ang-1), a

ligand for the Tie2 receptor tyrosine kinase which forms an important endothelial signaling pathway that inhibits vascular permeability and leukocyte-endothelium interactions [21, 27, 28]. MSC EVs also contain a number of other factors such as hepatocyte growth factor (HGF), tissue inhibitor of metalloproteinase 3 (TIMP3), and sphingosine 1-phosphate (S1P), which have all been shown to have important roles in maintaining or restoring endothelial barrier function [28–30]. EVs from MSCs exposed to culture conditions mimicking an ischemic microenvironment have also been found to contain an abundance of proteins involved in pathways including vascular wall cell surface interactions, cadherin signaling, cytoskeletal signaling, and vasculogenesis [31].

There are several important limitations to this study. First, the Caco-2 cell line used in vitro is derived from colon adenocarcinoma, which may not entirely reflect the response of the small intestine to oxidative stress in vivo. However, the Caco-2 cell line in culture resembles enterocytes lining the small intestine, is used extensively to study the intestinal epithelial barrier, and is considered the in vitro gold standard for the assessment of drug permeability and absorption [32]. Second, human rather than mouse MSCs and MSC EVs were used in a mouse model, which raises the possibility

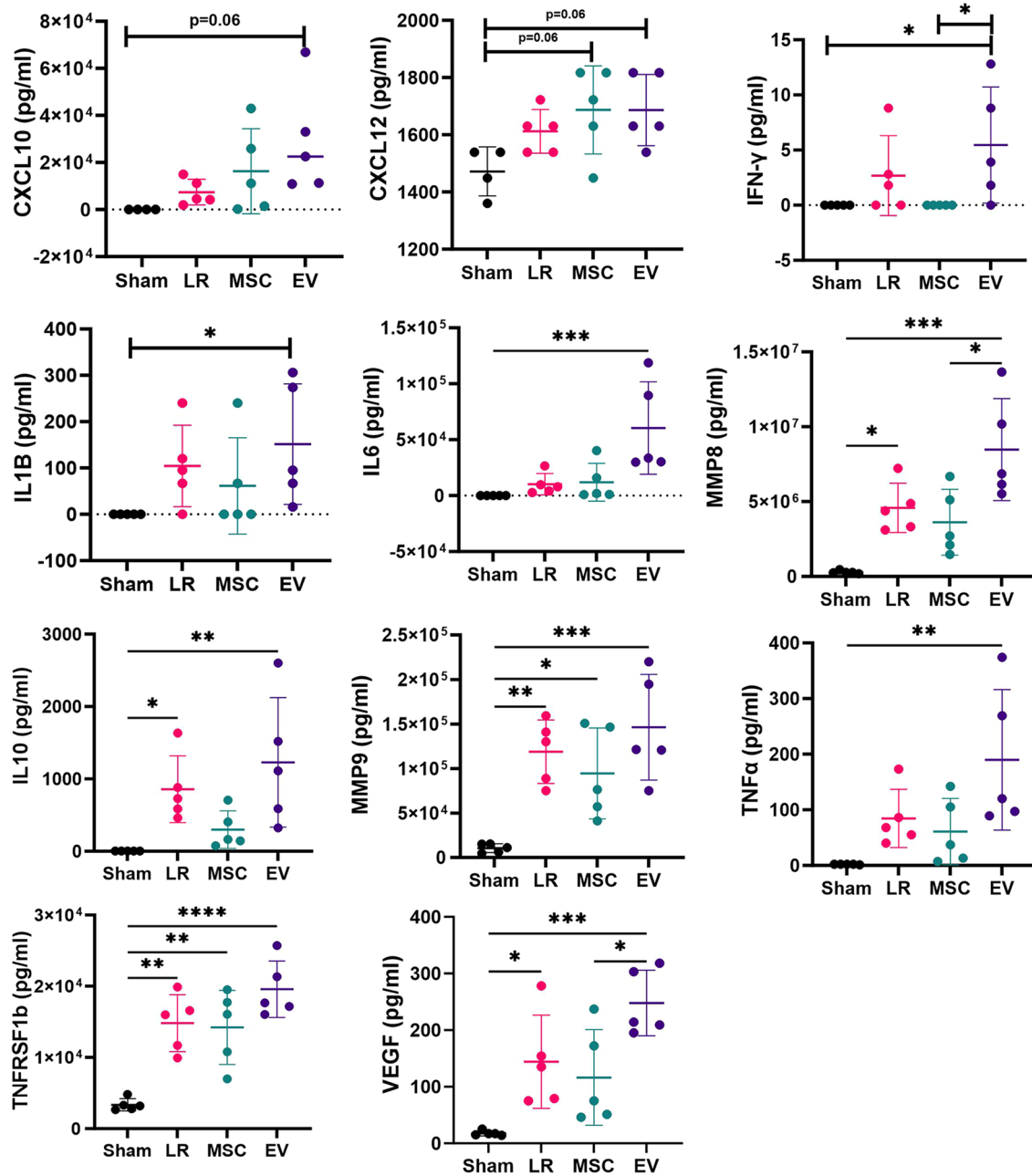


Fig. 6 Plasma Biomarker Analysis. Plasma biomarkers of inflammation and endothelial function were evaluated using a custom Luminex[®] assay (N=5 mice per group). Only biomarkers with significant differences between groups are shown here. Groups were compared using one-way ANOVA for normally distributed data and Kruskal–Wallis testing for data that were not normally distributed. Outliers were defined by the GraphPad program and were removed from analysis. Measurements are expressed in pg/ml

of an interspecies effect. This was done to best evaluate the product that would be given to humans (i.e. human MSCs and MSC EVs). MSCs are also considered immune evasive and have been used in this manner in other studies [33]. Third, because there were no changes in tight junction staining in the intestinal

epithelial barrier in vivo, we were unable to determine the impact of these therapies on the gut barrier. This was an unexpected finding given the clear decrease in pulmonary epithelial tight junction staining after HS/T, and others have demonstrated loss of intercellular junction integrity in the gut in similar models [34–36].

Finally, a number of the plasma inflammatory biomarkers were unexpectedly not different between sham animal and the shocked groups, though this may not be surprising given that the sham animals in this study do undergo bilateral femoral artery cannulation and ligation, and therefore some degree of hindlimb ischemia, as well as 2 h of anesthetic time.

In conclusion, this study demonstrates that both MSCs and MSC EVs help to maintain vascular barrier integrity in vitro and in vivo in a mouse model of HS/T. MSC EVs may therefore be able to recapitulate many of the potential therapeutic benefits of MSCs in HS/T in a cell-free manner, overcoming some of the logistical barriers and disadvantages of live cell administration in patients. MSC-based therapies are currently being evaluated in a variety of clinical settings, with published trials demonstrating positive results and a favorable safety profile [37]. However, understanding the potential role of these therapies in HS/T is only in its infancy [9, 38]. A number of questions remain to be addressed, including cell source, dosing, timing of delivery, and the duration of their effects. Further studies are also needed to validate MSC-based therapies in critically ill patients with systemic inflammation and coagulopathy and in patients who are receiving simultaneous therapies such as blood products and hemostatic agents.

Supplementary Information

The online version contains supplementary material available at <https://doi.org/10.1186/s12967-024-05406-1>.

Supplementary Material 1.

Acknowledgements

Not applicable.

Author contributions

All authors participated in manuscript preparation and revision. MB—planning, performed the experiments, data analysis, manuscript drafting. AT—planning, data analysis, data interpretation. BM—planning, performed the experiments, data analysis, PP—performed the experiments, LV—performed the experiments, DS—performed the experiments, JC—planning, manuscript revision, SP—supervision, planning, data interpretation.

Funding

Funding for this work was provided by NIH Grant R01GM111899.

Availability of data and materials

The datasets used and/or analyzed during the current study are available from the corresponding author on reasonable request.

Declarations

Ethics approval and consent to participate

Animal studies were performed with approval of the Institutional Animal Care and Use Committee (IACUC) at UCSF. The experiments were conducted in compliance with the ARRIVE guidelines for animal models and the National Institutes of Health (NIH) guidelines on the use of laboratory animals.

Consent for publication

Not applicable.

Competing interests

The authors declare that they have no competing interests.

Received: 17 April 2024 Accepted: 14 June 2024

Published online: 21 June 2024

References

- Jenkins DH, Rappold JF, Badloe JF, et al. Trauma hemostasis and oxygenation research position paper on remote damage control resuscitation: definitions, current practice, and knowledge gaps. *Shock*. 2014;41(Suppl 1):3–12. <https://doi.org/10.1097/SHK.0000000000000140>.
- Holcomb JB, Pati S. Optimal trauma resuscitation with plasma as the primary resuscitative fluid: the surgeon's perspective. *Hematology Am Soc Hematol Educ Program*. 2013;2013:656–9. <https://doi.org/10.1182/asheducation-2013.1.656>.
- Barry M, Pati S. Targeting repair of the vascular endothelium and glyco-calyx after traumatic injury with plasma and platelet resuscitation. *Matrix Biol Plus*. 2022;14: 100107. <https://doi.org/10.1016/j.mbplus.2022.100107>.
- Naumann DN, Hazeldine J, Davies DJ, et al. Endotheliopathy of trauma is an on-scene phenomenon, and is associated with multiple organ dysfunction syndrome: a prospective observational study. *Shock*. 2018;49(4):420–8. <https://doi.org/10.1097/SHK.0000000000000999>.
- Johansson PI, Henriksen HH, Stensballe J, et al. Traumatic endotheliopathy: a prospective observational study of 424 severely injured patients. *Ann Surg*. 2017;265(3):597–603. <https://doi.org/10.1097/SLA.00000000000001751>.
- Langan NR, Eckert M, Martin MJ. Changing patterns of in-hospital deaths following implementation of damage control resuscitation practices in US forward military treatment facilities. *JAMA Surg*. 2014;149(9):904–12. <https://doi.org/10.1001/jamasurg.2014.940>.
- Cannon JW, Khan MA, Raja AS, et al. Damage control resuscitation in patients with severe traumatic hemorrhage: a practice management guideline from the Eastern Association for the Surgery of Trauma. *J Trauma Acute Care Surg*. 2017;82(3):605–17. <https://doi.org/10.1097/TA.0000000000001333>.
- Centers for Disease Control and Prevention, National Center for Injury Prevention and Control. Web-based Injury Statistics Query and Reporting System (WISQARS). Accessed May 16, 2022. www.cdc.gov/injury/wisqars.
- Pati S, Pilia M, Grimsley JM, et al. Cellular therapies in trauma and critical care medicine: forging new frontiers. *Shock*. 2015;44(6):505–23. <https://doi.org/10.1097/SHK.0000000000000482>.
- Matthay MA, Pati S, Lee JW. Concise review: mesenchymal stem (stromal) cells: biology and preclinical evidence for therapeutic potential for organ dysfunction following trauma or sepsis. *Stem Cells*. 2017;35(2):316–24. <https://doi.org/10.1002/stem.2551>.
- Pati S, Gerber MH, Menge TD, et al. Bone marrow derived mesenchymal stem cells inhibit inflammation and preserve vascular endothelial integrity in the lungs after hemorrhagic shock. *PLoS ONE*. 2011;6(9): e25171. <https://doi.org/10.1371/journal.pone.0025171>.
- Barry M, Trivedi A, Pathipati P, et al. Mesenchymal stem cell extracellular vesicles mitigate vascular permeability and injury in the small intestine and lung in a mouse model of hemorrhagic shock and trauma. *J Trauma Acute Care Surg*. 2022;92(3):489–98. <https://doi.org/10.1097/TA.00000000000003487>.
- Aussel C, Baudry N, Grosbot M, et al. IL-1 β primed mesenchymal stromal cells moderate hemorrhagic shock-induced organ injuries. *Stem Cell Res Ther*. 2021;12(1):438. <https://doi.org/10.1186/s13287-021-02505-4>.
- Zhang Y, Zhang X, Zhang H, et al. Mesenchymal stem cells derived extracellular vesicles alleviate traumatic hemorrhagic shock induced hepatic injury. *Front Immunol*. 2021;12: 811164. <https://doi.org/10.3389/fimmu.2021.811164>.
- Gore AV, Bible LE, Livingston DH, Mohr AM, Sifri ZC. Mesenchymal stem cells reverse trauma and hemorrhagic shock-induced bone marrow dysfunction. *J Surg Res*. 2015;199(2):615–21. <https://doi.org/10.1016/j.jss.2015.06.023>.

16. Eggenhofer E, Luk F, Dahlke MH, Hoogduijn MJ. The life and fate of mesenchymal stem cells. *Front Immunol*. 2014;5:148. <https://doi.org/10.3389/fimmu.2014.00148>.
17. Rani S, Ryan AE, Griffin MD, Ritter T. Mesenchymal stem cell-derived extracellular vesicles: toward cell-free therapeutic applications. *Mol Ther*. 2015;23(5):812–23. <https://doi.org/10.1038/mt.2015.44>.
18. Raposo G, Stahl PD. Extracellular vesicles: a new communication paradigm? *Nat Rev Mol Cell Biol*. 2019;20(9):509–10. <https://doi.org/10.1038/s41580-019-0158-7>.
19. Baek G, Choi H, Kim Y, Lee HC, Choi C. Mesenchymal stem cell-derived extracellular vesicles as therapeutics and as a drug delivery platform. *Stem Cells Transl Med*. 2019;8(9):880–6. <https://doi.org/10.1002/sctm.18-0226>.
20. Barry M, Trivedi A, Miyazawa BY, et al. Cryoprecipitate attenuates the endotheliopathy of trauma in mice subjected to hemorrhagic shock and trauma. *J Trauma Acute Care Surg*. 2021. <https://doi.org/10.1097/TA.0000000000003164>.
21. Potter DR, Miyazawa BY, Gibb SL, et al. Mesenchymal stem cell-derived extracellular vesicles attenuate pulmonary vascular permeability and lung injury induced by hemorrhagic shock and trauma. *J Trauma Acute Care Surg*. 2018;84(2):245–56. <https://doi.org/10.1097/TA.0000000000001744>.
22. Kumar H, Jo MJ, Choi H, et al. Matrix metalloproteinase-8 inhibition prevents disruption of blood-spinal cord barrier and attenuates inflammation in rat model of spinal cord injury. *Mol Neurobiol*. 2018;55(3):2577–90. <https://doi.org/10.1007/s12035-017-0509-3>.
23. Bates DO. Vascular endothelial growth factors and vascular permeability. *Cardiovasc Res*. 2010;87(2):262–71. <https://doi.org/10.1093/cvr/cvq105>.
24. Hoogduijn MJ, Roemeling-van Rhijn M, Engela AU, et al. Mesenchymal stem cells induce an inflammatory response after intravenous infusion. *Stem Cells Dev*. 2013;22(21):2825–35. <https://doi.org/10.1089/scd.2013.0193>.
25. Kou M, Huang L, Yang J, et al. Mesenchymal stem cell-derived extracellular vesicles for immunomodulation and regeneration: a next generation therapeutic tool? *Cell Death Dis*. 2022;13(7):580. <https://doi.org/10.1038/s41419-022-05034-x>.
26. Gao F, Chiu SM, Motan DA, et al. Mesenchymal stem cells and immunomodulation: current status and future prospects. *Cell Death Dis*. 2016;7(1):e2062. <https://doi.org/10.1038/cddis.2015.327>.
27. Saharinen P, Eklund L, Alitalo K. Therapeutic targeting of the angiotensin-TIE pathway. *Nat Rev Drug Discov*. 2017;16(9):635–61. <https://doi.org/10.1038/nrd.2016.278>.
28. Hu S, Park J, Liu A, et al. Mesenchymal stem cell microvesicles restore protein permeability across primary cultures of injured human lung microvascular endothelial cells. *Stem Cells Transl Med*. 2018;7(8):615–24. <https://doi.org/10.1002/sctm.17-0278>.
29. Wang H, Zheng R, Chen Q, Shao J, Yu J, Hu S. Mesenchymal stem cells microvesicles stabilize endothelial barrier function partly mediated by hepatocyte growth factor (HGF). *Stem Cell Res Ther*. 2017;8(1):211. <https://doi.org/10.1186/s13287-017-0662-7>.
30. Menge T, Zhao Y, Zhao J, et al. Mesenchymal stem cells regulate blood-brain barrier integrity through TIMP3 release after traumatic brain injury. *Sci Transl Med*. 2012;4(161):161ra50. <https://doi.org/10.1126/scitranslmed.3004660>.
31. Anderson JD, Johansson HJ, Graham CS, et al. Comprehensive proteomic analysis of mesenchymal stem cell exosomes reveals modulation of angiogenesis via nuclear factor-KappaB signaling. *Stem Cells*. 2016;34(3):601–13. <https://doi.org/10.1002/stem.2298>.
32. Sambuy Y, De Angelis I, Ranaldi G, Scarino ML, Stamatii A, Zucco F. The Caco-2 cell line as a model of the intestinal barrier: influence of cell and culture-related factors on Caco-2 cell functional characteristics. *Cell Biol Toxicol*. 2005;21(1):1–26. <https://doi.org/10.1007/s10565-005-0085-6>.
33. Ankrum JA, Ong JF, Karp JM. Mesenchymal stem cells: immune evasive, not immune privileged. *Nat Biotechnol*. 2014;32(3):252–60. <https://doi.org/10.1038/nbt.2816>.
34. Schucht JE, Matheson PJ, Harbrecht BG, Bond L, Ashkettle GR, Smith JW. Plasma resuscitation with adjunctive peritoneal resuscitation reduces ischemia-induced intestinal barrier breakdown following hemorrhagic shock. *J Trauma Acute Care Surg*. 2021;90(1):27–34. <https://doi.org/10.1097/TA.0000000000002916>.
35. Thuijls G, de Haan JJ, Derikx JP, et al. Intestinal cytoskeleton degradation precedes tight junction loss following hemorrhagic shock. *Shock*. 2009;31(2):164–9. <https://doi.org/10.1097/SHK.0b013e31817fc310>.
36. Yang R, Han X, Uchiyama T, et al. IL-6 is essential for development of gut barrier dysfunction after hemorrhagic shock and resuscitation in mice. *Am J Physiol Gastrointest Liver Physiol*. 2003;285(3):G621–9. <https://doi.org/10.1152/ajpgi.00177.2003>.
37. Rodríguez-Fuentes DE, Fernández-Garza LE, Samia-Meza JA, Barrera-Barrera SA, Caplan AI, Barrera-Saldaña HA. Mesenchymal stem cells current clinical applications: a systematic review. *Arch Med Res*. 2021;52(1):93–101. <https://doi.org/10.1016/j.arcmed.2020.08.006>.
38. Herzig MC, Cap AP. Challenges in translating mesenchymal stem cell therapies for trauma and critical care. *Transfusion*. 2016;56(4):20S–S25. <https://doi.org/10.1111/trf.13566>.

Publisher's Note

Springer Nature remains neutral with regard to jurisdictional claims in published maps and institutional affiliations.